NeuroImage 66 (2013) 469–478

Contents lists available at SciVerse ScienceDirect

NeuroImage

journal homepage: www.elsevier.com/locate/ynimg

Crossmodal bias of visual input on pain perception and pain-induced beta activity

Ulrich Pomper [a,b,*], Marion Höfle [a,b], Michael Hauck [a,c], Norbert Kathmann [d], Andreas K. Engel [a], Daniel Senkowski [a,b]

[a] Department of Neurophysiology and Pathophysiology, University Medical Center Hamburg-Eppendorf, Martinistr. 52, 20246 Hamburg, Germany
[b] Department of Psychiatry and Psychotherapy, Charité University Medicine Berlin, St. Hedwig Hospital, Große Hamburger Str. 5-11, 10115 Berlin, Germany
[c] Department of Neurology, University Medical Center Hamburg-Eppendorf, Martinistr. 52, 20246 Hamburg, Germany
[d] Department of Psychology, Humboldt-Universität zu Berlin, Rudower Chaussee 18, 12489 Berlin, Germany

ARTICLE INFO

Article history:
Accepted 4 October 2012
Available online 27 October 2012

Keywords:
Multisensory
EEG
Neural synchrony
Oscillations
Event-related potentials
Gamma-band

ABSTRACT

In our environment, acute pain is often accompanied by input from other sensory modalities, like visual stimuli, which can facilitate pain processing. To date, it is not well understood how these inputs influence the perception and processing of pain. Previous studies on integrative processing between sensory modalities other than pain have shown that multisensory response gains are strongest when the constituent unimodal stimuli are minimally effective in evoking responses. This finding has been termed the principle of *inverse effectiveness* (IE). In this high-density electroencephalography study, we investigated the influence of Gabor patches of low and high contrast levels on the perception and processing of spatially and temporally aligned painful electrical stimuli of low and high intensities. Subjective pain ratings, event-related potentials (ERPs) and oscillatory responses served as dependent measures. In line with the principle of IE, stronger crossmodal biasing effects of visual input on subjective pain ratings were found for low compared to high intensity painful stimuli. This effect was paralleled by stronger bimodal interactions in right-central ERPs (150–200 ms) for low compared to high intensity pain stimuli. Moreover, an enhanced suppression of medio-central beta-band activity (12–24 Hz, 200–400 ms) was found for low compared to high intensity pain stimuli. Our findings possibly reflect a facilitation of stimulus processing that serves to enhance response readiness of the sensorimotor system following painful stimulation. Taken together, our study demonstrates that multisensory processing between visual and painful stimuli follows the principle of IE and suggests a role for beta-band oscillations in the crossmodal modulation of pain.

Introduction

Acute pain often signals threat and potential damage to the individual, making fast and accurate processing of nociceptive input crucial for our survival. In our environment, pain often occurs together with information from other sensory modalities. Recent studies have shown that semantically meaningful visual stimuli, like emotional facial expressions (Senkowski et al., 2011a) or a needle pricking a hand (Höfle et al., 2012), influence the perception and processing of pain. Despite the high ecological relevance of pain, to date there is no detailed account of the interaction between nociception and vision, and how this interaction may be shaped by basic stimulus properties, such as stimulus intensity.

Research on multisensory integration has demonstrated that combining information across two or more sensory modalities often facilitates behavioral performance (Rach et al., 2011; Senkowski et al., 2011b) as well as neural responses (Stein and Stanford, 2008). A frequently observed effect in behavioral data is that perceived intensities of bimodal stimuli are increased compared to the perceived intensities of the corresponding unimodal stimuli (Frassinetti et al., 2002; Nasri et al., 2011; Odgaard et al., 2004; Stein et al., 1996). Stein et al. (1996) found that the presentation of a brief tone increases the perceived intensity of a concurrently presented flash. Similarly, Odgaard et al. (2004) demonstrated that bursts of white noise presented together with a light are perceived as being louder than noise presented alone. Paralleling these behavioral findings, human neurophysiological studies have shown enhanced neural activity in response to bimodal compared to the corresponding unimodal stimuli (Giard and Peronnet, 1999; Gondan et al., 2005; Murray et al., 2005; Talsma and Woldorff, 2005).

A hallmark of multisensory processing is that the magnitude of behavioral facilitation, as well as the modulation of neural activity, is often inversely related to the intensity of the presented stimuli. Bimodal stimuli more frequently lead to stronger facilitation effects when the constituent unimodal stimuli are low in intensity compared to when they are high in intensity (Corneil et al., 2002; Diederich and Colonius, 2004; Rach et al., 2011). This so called principle of *inverse effectiveness* (IE) was first shown in single neuron recordings from

* Corresponding author at: Department of Psychiatry and Psychotherapy, Charité University Hospital, St. Hedwig Hospital, Grosse Hamburger Strasse 5-11, 10115 Berlin, Germany. Fax: +49 3023112209.
E-mail address: ulrich.pomper@charite.de (U. Pomper).

1053-8119/$ – see front matter © 2012 Elsevier Inc. All rights reserved.
http://dx.doi.org/10.1016/j.neuroimage.2012.10.040

the cat superior colliculus (Stein and Meredith, 1993) and has recently been demonstrated in a number of human behavioral and neurophysiological studies (Cappe et al., 2012; Senkowski et al., 2011b; Stevenson and James, 2009; Stevenson et al., 2012; but see Ross et al., 2007). Whether IE also applies to the interaction of painful and visual stimuli is thus far unknown.

A candidate neural mechanism that could be crucial for integrative processing of visual and painful stimuli is neural synchrony. Human electroencephalography (EEG) and magnetoencephalography (MEG) studies have highlighted the critical role of synchronized oscillatory activity in both pain processing (Hauck et al., 2008) and multisensory integration (Kayser et al., 2008; Senkowski et al., 2008). Pain processing under various experimental conditions has been shown to suppress oscillatory beta-band activity (BBA; 13–30 Hz) (Mancini et al., accepted for publication; Ploner et al., 2006; Raij et al., 2004; Senkowski et al., 2011a), in addition to modulations of low-frequency activity (2–12 Hz) (Domnick et al., 2009; Iannetti et al., 2008b; Mouraux et al., 2003) and high-frequency gamma-band activity (GBA; 30–100 Hz) (Gross et al., 2007; Hauck et al., 2007; Tiemann et al., 2010). The close relationship between pain processing and oscillatory responses indicates that the principle of IE, if applicable for integrative processing between painful and visual stimuli, may be reflected in modulations of oscillatory activity. In this EEG study, we investigated whether behavioral and neural interactions between visual and painful stimuli follow the principle of IE. We presented subjects with unimodal visual, unimodal painful and bimodal visual-painful stimuli of high and low intensities, while recording ERPs, oscillatory responses and subjective pain ratings.

Methods

Participants

Sixteen right-handed, paid volunteers participated in the study. Three participants had to be excluded because more than 50% of trials including painful stimulation had to be removed due to extensive muscle artifacts in their EEG data. The remaining thirteen participants (8 female, 20–31 years of age) had normal or corrected to normal vision and reported no history of neurological or psychiatric illness. All applied procedures were approved by the Ethics Commission of the Medical Association of Hamburg, Germany.

Stimuli and procedure

Nociceptive stimulation was realized by means of the intracutaneous electrical pain model (Bromm and Meier, 1984). Electrical stimuli (16 ms duration) were applied to the tip of participants' left index finger. To minimize the electrical artifact induced by the intracutaneous stimulation, a ground electrode was attached to the participants left wrist. Prior to the experimental session, individual pain thresholds were determined for each subject using a staircase procedure (Höfle et al., 2012). During the experiment, painful stimuli were presented with intensities of 1.2 and 1.5 fold individual pain threshold. We defined the former as low intensity and the latter as high intensity pain stimulus. Pilot studies showed that electrical stimuli of these intensities are consistently rated as painful. Visual stimuli consisted of black and white Gabor patches with vertical gratings (spatial frequency = 0.5 cycles per degree, Gaussian standard deviation = 150) and were presented for 100 ms. Stimulus intensity was manipulated by varying the contrast of Gabor patches while keeping the mean luminance constant at 26 cd/m^2. The Michelson contrast, i.e. [(luminance maximal − luminance minimal) / (luminance maximal + luminance minimal)] ∗ 100, for low and high intensity stimuli was 11 and 61, respectively. These intensities were selected in accordance with our recent study on the principle of IE in audiovisual processing (Senkowski et al., 2011b). Pain and visual stimuli were presented in a spatially congruent fashion (Fig. 1A). Participants placed their left hand beneath a tilted flat screen on which Gabor patches were centrally presented. The tip of participants' left index finger, to which the painful electrical stimulus was applied, was placed directly behind the Gabor patch. The experiment was conducted in an electrically shielded, sound proof, and dimly lit room. A continuous stream of randomized unimodal pain (P), unimodal visual (V) and bimodal (PV) trials was

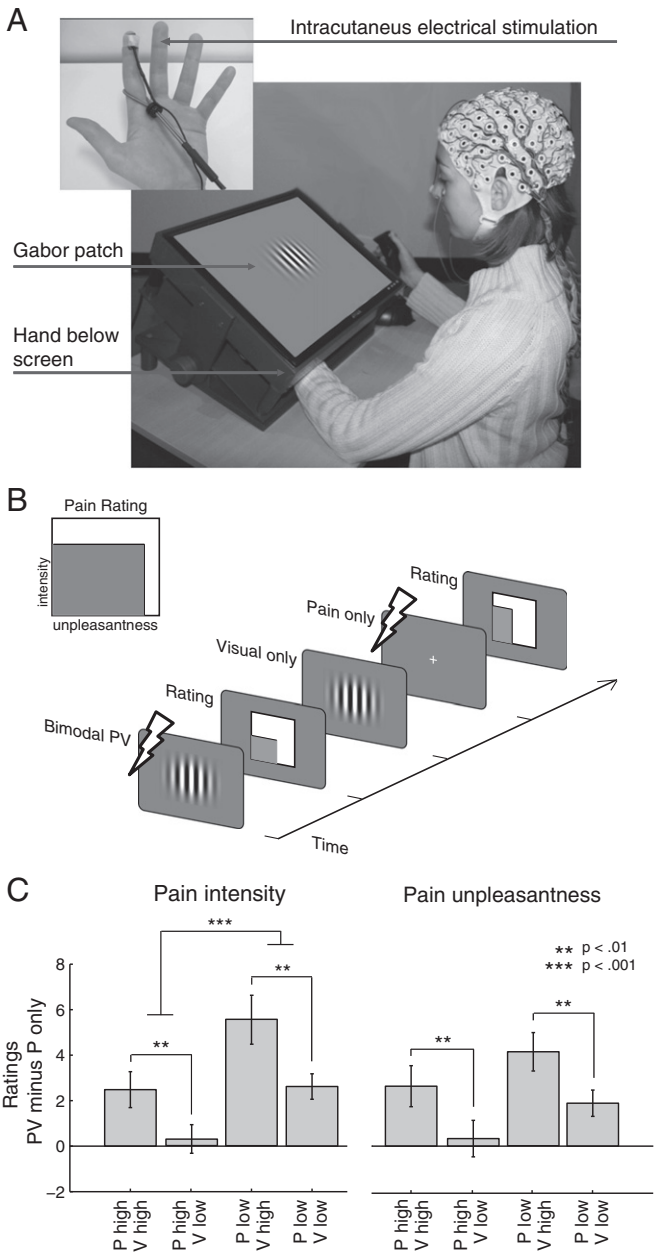

Fig. 1. Experimental setup. (A) Visual (Gabor-patches) and painful (intracutaneous electrical) stimuli were temporally and spatially aligned. Participants placed their left hand palm-upwards on a board beneath a tilted flat screen on which visual stimuli were presented. The tip of their left index finger, to which painful electrical stimuli were applied, was aligned with the center of the screen. (B) Center: Continuous stimulation stream. Participants were presented with a randomized stream of pain only (P), visual only (V), and bimodal painful-visual (PV) stimuli. After each pain stimulus, participants were asked to rate pain intensity and unpleasantness separately on a 2-dimensional scale using a joystick in their right hand. (C) Differences in pain intensity and unpleasant ratings for PV − P stimuli. Differences in intensity and unpleasantness ratings were larger for conditions with high compared to low visual stimulus intensities. A pattern of inverse effectiveness was found for the comparison between low versus high pain stimulus intensities. The crossmodal bias of visual input on pain ratings was stronger when painful stimuli were low compared to when they were high in intensity.

presented (Fig. 1B). Each stimulus modality was presented at low and high intensities, resulting in a total of four unimodal (P_{high}, P_{low}, V_{high}, and V_{low}) and four bimodal ($P_{high}V_{high}$, $P_{high}V_{low}$, $P_{low}V_{high}$, and $P_{low}V_{low}$) conditions. After the presentation of each electrical stimulus, participants rated *intensity* and *unpleasantness* of the experienced pain sensation on a 2-dimensional visual analog scale (VAS) using a joystick in their right hand (Fig. 1B). The VAS ranged between 0 and 100 on the vertical *intensity* axis (0 = no sensation, 40 = beginning of pain experience, as marked by a horizontal line, and 100 = highest imaginable pain) and between 0 and 100 on the horizontal *unpleasantness* axis (0 = not unpleasant at all and 100 = extremely unpleasant). To assure that participants attended to visual stimuli, catch trials consisting of horizontally oriented Gabor patches were intermingled with the regular trials at a total rate of 10.7%. Participants were instructed to indicate the appearance of a horizontal grating by a speeded button press on the joystick. Additionally, *no-stimulus* trials with 100 ms duration (analog to the duration of visual stimuli) were randomly intermixed into each block at a rate of 30%. No-stimulus trials were blank trials featuring neither painful nor visual stimuli. When presented at rates of about 30% these trials do not elicit physiological responses by themselves (Busse and Woldorff, 2003). The averaged response to no-stimulus trials contains the average overlapping activity from previous trials as well as anticipatory activity preceding the upcoming trial (Woldorff, 1993). These activities can be contaminating factors when the sum of two unimodal responses is compared with a single bimodal response (Teder-Sälejärvi et al., 2002). Subtracting the average no-stimulus trial activity from the responses to both unimodal and bimodal trials is an effective approach to control for these contaminating factors in the analysis of ERPs (Senkowski et al., 2007b; Talsma and Woldorff, 2005). All stimuli, including no-stimulus trials, were followed by inter-stimulus intervals (ISI), which varied randomly between 1000 and 1400 ms (mean 1200 ms). A white fixation cross was centrally presented on a gray background during ISI, pain-only, and no-stimulus trials. In total, 560 unimodal (280 P, 280 V), 560 bimodal PV, 480 no-stimulus, and 120 catch trials were presented. The experimental sessions consisted of 20 blocks comprising 86 trials each. Stimulus presentation was controlled using Presentation software (Neurobehavioral Systems, Albany CA).

EEG recording

EEG data were collected using a 126 channel system (Easycap, Falk Minow services). In addition, two electrodes were placed at the medial upper and lateral border of the right orbit to monitor eye movements. Data were recorded against nose reference with a pass band of 0.016–250 Hz and digitized with a sampling rate of 1000 Hz using a BrainAmp amplifier system (Brain Products). Analysis of the EEG data was performed using Matlab 7.3.0 (Math-Works), EEGLAB 5.03 (Delorme and Makeig, 2004), and FieldTrip (Oostenveld et al., 2011). During the off-line analysis, data were band pass filtered between 0.3 and 125 Hz, downsampled to 500 Hz, and re-referenced to common average. To remove line noise a narrow-band 50 Hz notch filter was applied. Channels with extremely high and/or low frequency artifacts throughout the entire recording were linearly interpolated (M = 4.8, ranging from 0 to 8 interpolated channels) using a model of the amplitude topography at the unit sphere surface based on all non-artifactual channels (Perrin et al., 1989). Epochs containing muscular or technical artifacts were removed after visual inspection. Next, an independent component analysis approach was applied to reduce artifacts such as eye-blinks, horizontal eye movements, electrocardiographic activity, as well as artifacts induced by the electrical stimulation. Independent components representing artifacts were removed from the EEG data by back-projecting all but these components (Schneider et al., 2008). Finally, all trials that still exceeded a threshold of 100 μV were rejected automatically. On average, 10.7% of trials were removed. Data were epoched from −500 ms before to 1000 ms after stimulus onset. Baselines were computed from −200 ms to 0 ms before trial onset for the ERP analysis, and from −300 ms to −100 ms before trial onset for the time–frequency analysis.

Data analysis

Pain ratings

Prior to statistical analysis, outlier trials in which intensity or unpleasantness ratings were above or below 2.5 SD of the individual subject and condition mean were removed from the dataset. The crossmodal bias on pain intensity and pain unpleasantness ratings was defined as the difference between pain ratings to bimodal PV stimuli minus pain ratings to unimodal P stimuli (i.e. PV − P). Since there were no pain ratings to V stimuli, a linear combination of P + V stimuli could not be calculated. For the statistical analysis, two-way repeated measures analyses of variance (ANOVAs) were performed separately on both, intensity and unpleasantness ratings (i.e. PV − P) using the factors condition (bimodal vs. combined unimodal) and stimulation ($P_{high}V_{high}$, $P_{high}V_{low}$, $P_{low}V_{high}$, and $P_{low}V_{low}$). Significant interactions were followed up by repeated measures ANOVAs using the factors visual contrast (high and low) and pain stimulus intensity (high and low).

Time–frequency analysis

Time–frequency representations (TFRs) for frequencies ranging from 2 to 30 Hz were calculated using Fast Fourier Transforms perform with Hanning tapered time windows (200 ms taper length, 5 Hz spectral smoothing). TFRs for frequencies ranging from 30 to 100 Hz were calculated using Fast Fourier Transform performed on a set of orthogonal Slepian tapers with 100 ms taper length and 10 Hz spectral smoothing (Mitra and Pesaran, 1999). Subsequently, all data were normalized by calculating the percent change to a −300 to −100 ms baseline as follows: $Pow(t,f)_{normalized} = 100 * (Pow(t,f)_{poststimulus} - Pow(f)_{baseline}) / Pow(f)_{baseline}$. Multisensory interactions in oscillatory responses were assessed by calculating the difference between total time–frequency responses to bimodal stimuli and combined unimodal stimuli. As phase information is not available in time–frequency space when power values are computed, merely summing up the averaged time–frequency responses to the unimodal pain and unimodal visual stimulation would result in an incorrect estimation of their joined activity (for a detailed discussion on this issue see Senkowski et al., 2007a). As suggested by Senkowski et al. (2007a), the sum of unimodal conditions was calculated at the single trial level prior to the time–frequency transformation. This allows for a cancelation of nociceptory and visually related oscillatory activity that is not aligned in phase. For each stimulation condition ($P_{high}V_{high}$, $P_{high}V_{low}$, $P_{low}V_{high}$, and $P_{low}V_{low}$), each unimodal V trial was combined with each unimodal P trial, resulting in a total of N (trials V) × M (trials P) combinations of trials per condition. Next, bimodal trials and combined unimodal trials were time–frequency transformed and multisensory interactions were calculated by contrasting bimodal with combined unimodal responses. This was done separately for each stimulation condition. Although the oscillatory responses to unimodal stimuli were not directly summed up, in the following sections we will refer to the combined unimodal oscillatory stimuli as P + V. For the analysis of BBA, a time–frequency window from 200 to 400 ms ranging from 12 to 24 Hz was used. This window was selected based on previous studies on pain processing (Senkowski et al., 2011a) and multisensory processing (Bauer et al., 2009; Trenner et al., 2008). Moreover, the selected time–frequency window fits with the main difference between bimodal and combined unimodal stimuli pooled across stimulus intensities (Supplementary Fig. 1A). Based on the topography of unimodal pain and unimodal visual responses, as well as on findings by previous studies (Babiloni et al., 2002; Bauer et al., 2009; Senkowski et al., 2011a), a medio-central and an occipital ROI (15 and 8 electrodes, respectively, Fig. 2B were selected for the analysis.

For the analysis of GBA, a time–frequency window from 50 to 250 ms ranging from 60 to 80 Hz was selected, in correspondence with previous studies on pain processing (Gross et al., 2007; Hauck et

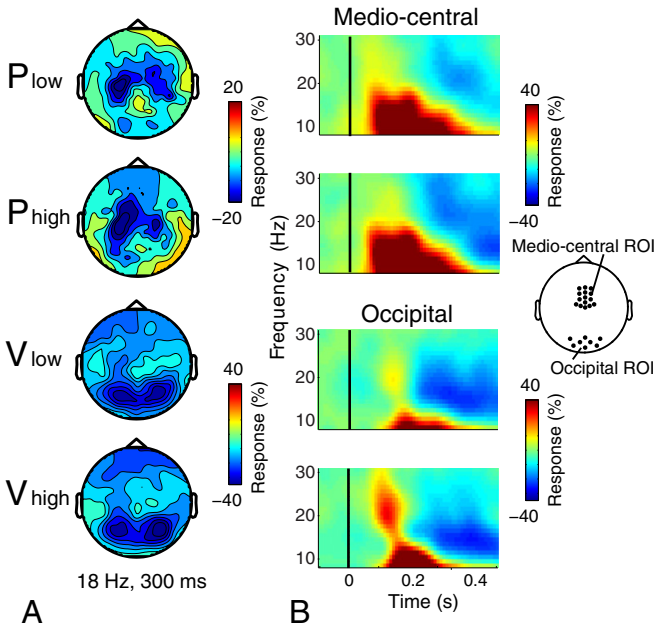

Fig. 2. Total oscillatory responses to unimodal painful and visual stimuli. (A) Topographical maps (300 ms, 18 Hz) for unimodal painful and unimodal visual stimuli of both low and high intensities. (B) Corresponding time–frequency representations (2–30 Hz) Strongest beta-band suppression was found at medio-central scalp for painful stimuli, and at occipital scalp for visual stimuli.

al., 2007; Senkowski et al., 2011a). Based on the topography of GBA to unimodal pain and unimodal visual stimuli (Supplemental Fig. 2), the analysis focused on the same medio-central and occipital ROIs as used for the analysis of BBA (Fig. 2B). The statistical analysis was conducted using a three-way repeated measures ANOVA with the factors condition (bimodal vs. combined unimodal), stimulation ($P_{high}V_{high}$, $P_{low}V_{high}$, $P_{high}V_{low}$, and $P_{low}V_{low}$) and ROI (medio-central vs. occipital). Significant interactions between condition and stimulation were followed up by ANOVAs on difference values (bimodal minus combined unimodal) using the factors visual contrast (high and low) and pain stimulus intensity (high and low).

Event-related potentials

The time-locked average of no-stimulus trials was removed from the ERPs of all unimodal and bimodal conditions prior to statistical analysis (see above). In line with previous studies (Giard and Peronnet, 1999; Molholm et al., 2002; Schneider et al., 2011), bimodal interactions in ERPs were assessed by directly comparing the neuronal responses to bimodal stimuli with the linear combination of responses to the respective unimodal stimuli (i.e. PV − (P + V)). In line with previous works on pain-related ERPs (Bromm and Meier, 1984; Legrain et al., 2009; Valeriani et al., 2008; but see also Iannetti et al., 2008a), our analysis focused on the N2/P2 complex peaking around 200 ms. Based on peak latencies found in our own data (Fig. 5A) as well as latencies reported by Mouraux et al. (2010), a time window from 150 to 200 ms (encompassing the N2) and a time window from 200 to 250 ms (encompassing the P2) were selected for further analysis. Based on the topography of the mean activity over all stimulus intensities (Supplemental Fig. 3), a right-central and a right-parietal ROI were defined for the statistical analysis. Three-way repeated measures ANOVAs with the factors condition (bimodal vs. combined unimodal), stimulation ($P_{high}V_{high}$, $P_{low}V_{high}$, $P_{high}V_{low}$, and $P_{low}V_{low}$), and ROI (right-central and right-parietal) were computed for both time windows. Significant interactions were followed up by two-way ANOVAs on difference values (PV − (P + V)), using the factors visual contrast (high and low) and pain stimulus intensity (high and low).

Results

Behavioral data

ANOVAs were calculated for intensity and unpleasantness ratings using the factors condition (bimodal vs. combined unimodal) and stimulation ($P_{high}V_{high}$, $P_{low}V_{high}$, $P_{high}V_{low}$, and $P_{low}V_{low}$). The ANOVA for intensity ratings (Table 1) revealed significant main effects of condition ($F_{1,12} = 17.38$, $p \leq 0.001$), stimulation ($F_{3,12} = 25.19$, $p \leq 0.001$), as well as a significant interaction between these factors ($F_{3,36} = 23.02$, $p \leq 0.001$). A two-way follow-up ANOVA was conducted on difference values (PV − P) using the factors visual contrast and pain stimulus intensity (Fig. 1C). The ANOVA revealed a significant main effect of visual contrast ($F_{1,12} = 23.58$, $p \leq 0.001$), indicating larger rating differences for high contrast (M = 4.02) compared to low contrast visual stimuli (M = 1.45). In addition, a significant main effect of pain stimulus intensity

Table 1
Analysis of variance for behavioral data, ERPs and oscillatory responses.

	df	Intensity		Unpleasantness		Beta-band		Gamma-band		ERP 150–200 ms		ERP 200–250 ms	
		F	*P*-value	F	*P*-value	F	*P*-value	F	*P*-value	F	*P*-value	F	*P*-value
Condition (Cond)	1,12	17.38	**0.001*****	18.67	**0.001*****	9.15	**0.011***	14.91	**0.002****	1.65	0.224	0.11	0.748
Stimulation (Stim)	3,12	25.19	**0.000*****	38.52	**0.000*****	1.06	0.377	3.86	**0.017***	0.22	0.881	8.21	**0.000*****
ROI	1,12	–	–	–	–	2.25	0.160	0.06	0.805	2.74	0.124	20.5	**0.000*****
Cond × Stim	3,36	23.02	**0.000*****	38.42	**0.000*****	2.22	0.103	1.44	0.247	3.05	**0.041***	1.31	0.285
Cond × ROI	3,36	–	–	–	–	6.96	**0.022***	0.02	0.896	8.00	**0.015***	1.06	0.323
Stim × ROI	3,36	–	–	–	–	3.06	**0.040***	0.15	0.923	12.77	**0.000*****	0.63	0.602
Cond × Stim × ROI	3,36	–	–	–	–	4.73	**0.007****	0.30	0.825	0.269	0.847	0.20	0.899

	df	Intensity		Unpleasantness		Beta-band central		Beta-band occipital		ERP[a] anterior		ERP[a] posterior	
		F	*P*-value	F	*P*-value	F	*P*-value	F	*P*-value	F	*P*-value	F	P-value
Pain level	1,12	18.36	**0.001*****	2.99	0.11	6.77	**0.023***	3.29	0.095	7.46	**0.012***	1.18	0.300
Contrast level	1,12	23.58	**0.000*****	10.05	**0.008****	3.35	0.092	2.87	**0.049***	2.16	0.168	0.05	0.831
Pain × contrast level	3,36	3.56	0.084	0.01	0.932	0.36	0.561	0.97	0.410	0.92	0.356	0.79	0.391

* $p \leq 0.05$.
** $p \leq 0.01$.
*** $p \leq 0.001$.
[a] 150–200 ms.
Significant results highlighted in bold.

was found ($F_{1,12} = 18.36$, $p \leq 0.001$), due to higher rating differences for low intensity ($M = 4.09$) compared to high intensity ($M = 1.38$) painful stimuli, a finding that is in line with the principle of IE. The ANOVA for unpleasantness ratings (Table 1) revealed significant main effects of condition ($F_{1,12} = 18.67$, $p \leq 0.001$) and stimulation ($F_{3,12} = 38.52$, $p \leq 0.001$), as well as a significant interaction between these factors ($F_{3,36} = 38.42$, $p \leq 0.001$). The follow-up two-way ANOVA revealed a significant main effect of visual contrast ($F_{1,12} = 10.05$, $p \leq 0.008$), with larger differences for high contrast (average difference = 3.38) compared to low contrast (average difference = 1.11) stimuli. It was also found that mean unpleasantness rating differences were larger for low intensity compared to high intensity pain stimuli, however, this effect was not significant ($F_{1,12} = 2.99$, $p \leq 0.11$). Finally, participants correctly detected 91.6% of the visual catch trials (range 70.5–100%), indicating that visual attention during the experiment was directed to the Gabor patches.

Beta-band activity

Fig. 2 illustrates TFRs and topographical maps of BBA after unimodal painful and visual stimulation. Starting around 200 ms after stimulus onset, painful stimulation caused an enhanced suppression of BBA at medio-central scalp regions, encompassing areas over the sensorimotor cortex. For visual stimulation, the strongest suppression of BBA was found at posterior scalp, encompassing areas of visual cortex. Fig. 3 shows TFRs of bimodal and the combined unimodal stimuli, as well as their difference. The figure indicates differences between bimodal and combined unimodal stimuli around 300 ms after the stimulus onset in the beta-band (~18 Hz). These effects differed between the different intensity conditions, especially at medio-central and occipital scalp (Fig. 4). The three-way ANOVA for BBA (200–400 ms, 12–24 Hz; Table 1) with the factors condition, stimulation, and ROI revealed a significant main effect of condition ($F_{1,12} = 9.15$, $p \leq 0.011$) and significant interactions between the factors condition and ROI ($F_{3,36} = 6.96$, $p \leq 0.022$) and stimulation and ROI ($F_{3,36} = 3.06$, $p \leq 0.04$). Moreover, a three-way interaction between condition, stimulation and ROI was found ($F_{3,36} = 4.73$, $p \leq 0.007$). Follow-up two-way ANOVAs were conducted separately for each ROI using the differences between bimodal and combined unimodal responses as dependent variable and the factors visual contrast (high and low) and pain stimulus intensity (high and low) as independent variables. The ANOVA for the medio-central ROI revealed

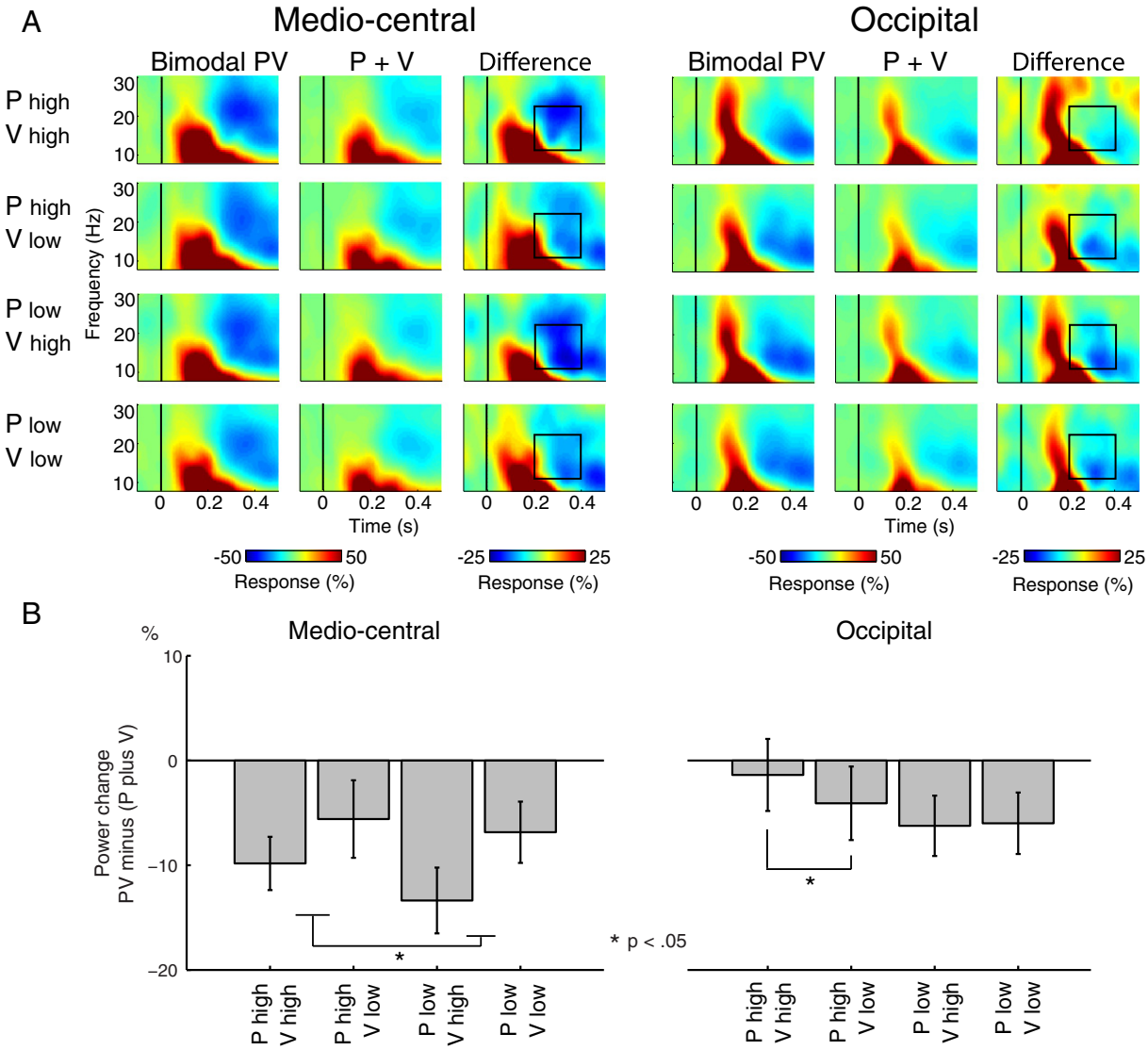

Fig. 3. Time–frequency representations of total beta-band oscillatory activity (2–30 Hz) to bimodal visual-painful and combined painful and visual trials. (A) Time–frequency representations of bimodal (left column), combined unimodal (middle column), and differences between bimodal and combined unimodal responses (right column) for all stimulus conditions at medio-central (left panel) and occipital (right panel) scalp. (B) Differences in power change (bimodal minus combined unimodal) at medio-central and occipital ROIs for the time–frequency window of 200–400 ms and 12–24 Hz. Left panel: Suppression of beta-band activity at medio-central scalp was stronger for low compared to high pain stimuli. Right panel: Suppression of beta-band activity at occipital scalp was significantly larger for low compared to high intensity visual stimuli.

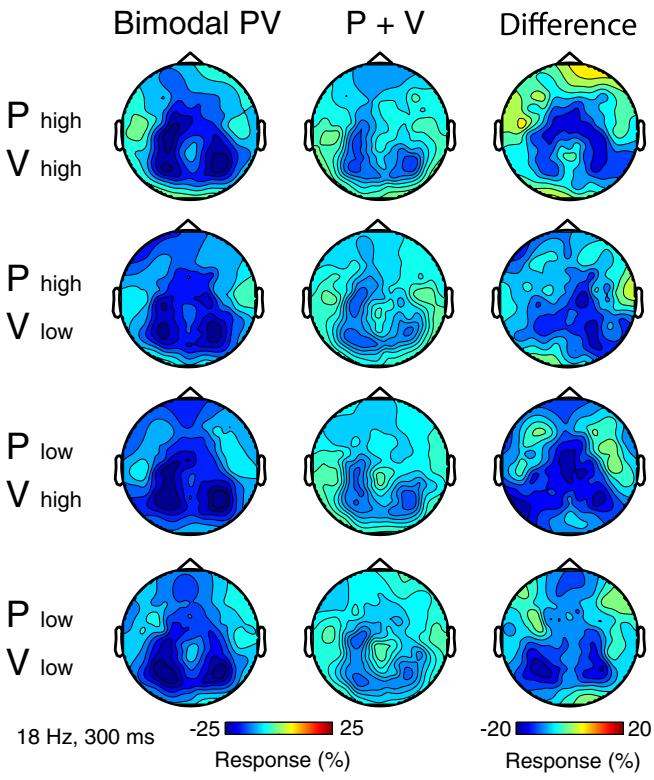

Fig. 4. Topographical maps (300 ms, 18 Hz) for bimodal (left column) and combined unimodal responses (middle column), as well as their differences (right column). Robust suppression of beta-band activity was observed at medio-central and occipital scalp. Suppression of beta-band activity at the medio-central ROI was significantly larger for low compared to high pain stimuli. Power changes at the occipital ROI were significantly larger for low compared to high intensity visual stimuli.

a significant main effect of pain stimulus intensity ($F_{1,12} = 6.77$, $p \leq 0.023$), due to larger response differences for stimuli containing low compared to high intensity painful input. At the occipital ROI, a significant main effect of visual contrast was found ($F_{1,12} = 2.87$, $p \leq 0.049$), due to larger response differences for stimuli containing low compared to high contrast visual inputs. Thus, the effect of pain stimulus intensity on medio-central BBA suppression and the effect of visual stimulus intensity on occipital BBA suppression were both in line with the principle of IE.

Gamma-band activity

Fig. 5A illustrates TFRs of GBA in response to bimodal visual-painful and combined unimodal stimuli, as well as their difference. The figure indicates differences between responses to bimodal and combined unimodal stimulation around 150 ms after the stimulus onset. Fig. 5B shows the topography of the gamma-band response, encompassing medio-central as well as occipital regions largely similar to the beta-band response. The three-way ANOVA for GBA (50–250 ms, 60–80 Hz) using the factors condition, stimulation, and ROI revealed a significant main effect of condition ($F_{1,12} = 14.91$, $p \leq 0.002$), due to larger responses for bimodal compared to combined unimodal stimuli. Moreover, a significant main effect of stimulation ($F_{3,36} = 3.86$, $p \leq 0.017$) was found, with high intensity stimuli eliciting larger responses than low intensity stimuli. No further significant main effects or interactions were found.

Event-related potentials

The ERPs showed a typical N2/P2 complex, which was similar for bimodal and combined unimodal conditions. Fig. 6A indicates early differences between bimodal and combined unimodal conditions for the

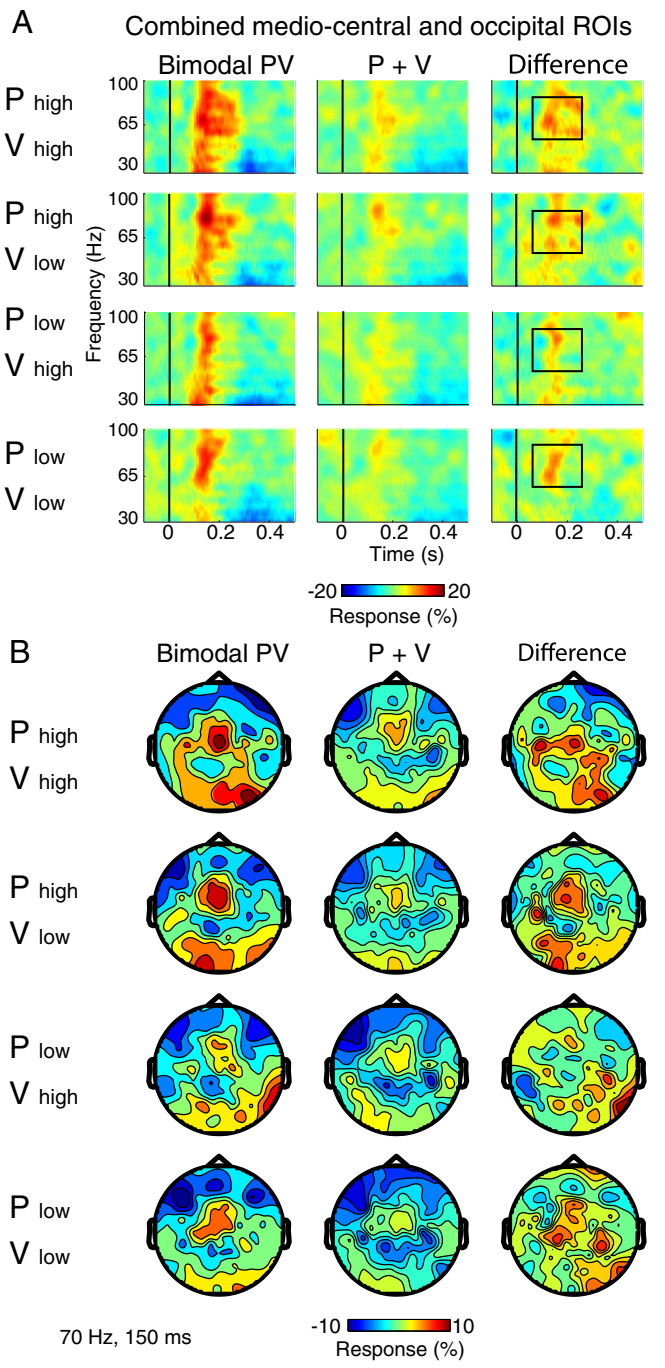

Fig. 5. Gamma-band responses. (A) Time–frequency representations of bimodal (left column), combined unimodal (middle column), and differences between bimodal and combined unimodal responses (right column) for all stimulus conditions. Whereas overall gamma-band responses were larger when stimulus intensities were high, there was no effect of stimulus intensity on the difference between bimodal and combined unimodal responses. (B) Corresponding topographical maps (70 Hz, 150 ms).

N2 component around 150–200 ms. Across conditions, N2 amplitudes were larger for bimodal compared to combined unimodal trials, indicative of super-additive multisensory interactions. For the 150–200 ms time-window (encompassing the N2 component; Table 1) the three-way ANOVA using the factors condition (bimodal vs. combined unimodal), stimulation ($P_{high}V_{high}$, $P_{low}V_{high}$, $P_{high}V_{low}$, and $P_{low}V_{low}$) and ROI (right-central and right-parietal) revealed a significant interaction between condition and stimulation ($F_{3,36} = 3.05$, $p \leq 0.041$), a significant interaction between condition and ROI ($F_{3,36} = 8.00$, $p \leq 0.015$), as

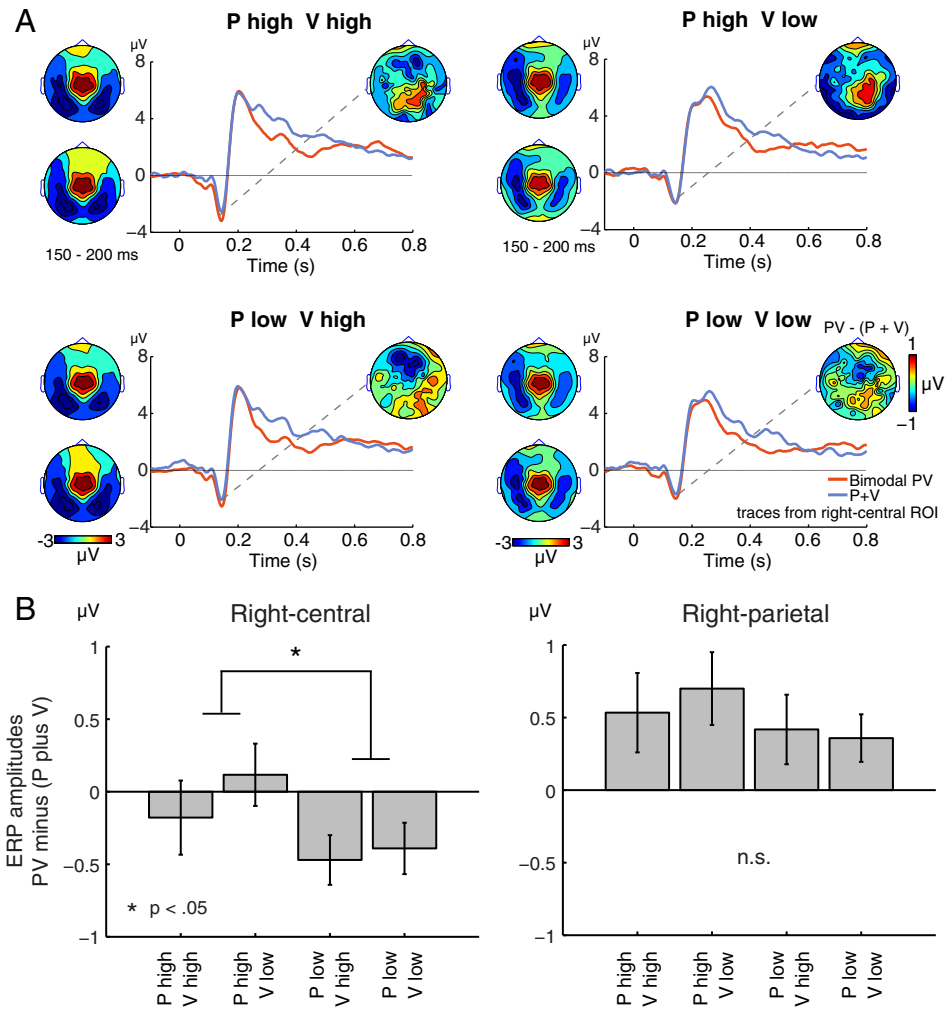

Fig. 6. Event related potentials. (A) ERP amplitude traces and topographical maps for the 150–200 ms time-window for each of the four bimodal and combined unimodal stimulation conditions. (B) Differences in ERP mean amplitudes between bimodal and combined unimodal conditions for the 150–200 ms time window. Amplitude differences at the right-central scalp were significantly larger for low intensity pain compared to high intensity pain stimuli.

well as a significant interaction between stimulation and ROI ($F_{3,\ 36} = 12.77$, $p \leq 0.000$). Follow-up two-way ANOVAs were conducted on the amplitude differences between bimodal and combined unimodal stimuli for each ROI separately using the factors visual contrast (high and low) and pain stimulus intensity (high and low). The ANOVA for the right-central ROI revealed a significant main effect for pain intensity ($F_{1,12} = 7.46$, $p \leq 0.012$), due to larger amplitude differences for the low compared to the high painful stimulation (Fig. 6B). This finding further supports the notion that the principle of IE applies to the multisensory processing of painful stimuli. No significant effects were found for the right-parietal ROI (Fig. 6B). The ANOVA for the 200–250 ms time-window (encompassing the P2 component) revealed a significant main effect for stimulation ($F_{1,12} = 8.21$, $p \leq 0.000$) as well as a significant main effect for ROI ($F_{1,12} = 20.50$, $p \leq 0.000$). No further significant effects were found.

Discussion

In this study, we investigated the effect of stimulus intensity on multisensory processing between spatially and temporally aligned painful and visual stimuli. As a main result, we found that the crossmodal bias of visual stimuli on pain intensity ratings and neural processing in BBA and ERPs follows the principle of IE.

Pain ratings

In agreement with the principle of IE the crossmodal bias of visual inputs was stronger on low compared to high intensity painful stimuli. Behavioral studies in humans have previously shown that the principle of IE is applicable to multisensory processing between various modalities other than pain. Using reaction times as dependent variable, IE has been shown for audiovisual processing (Corneil et al., 2002; Senkowski et al., 2011b; Stevenson et al., 2012; but see Ross et al., 2007) as well as for audio-tactile and visual-tactile processing (Diederich and Colonius, 2004). In addition, IE has also been reported for detection rates in audiovisual processing (Rach et al., 2011). Our results are in line with these findings and extend them by showing that the IE is also applicable to the crossmodal influence of visual inputs on perceived pain intensity.

While the crossmodal bias of pain perception by concurrent visual stimuli was inversely related to the strength of painful stimuli, we observed a stronger influence of high compared to low intensity visual stimuli on pain perception. Across conditions, the presentation of visual stimuli enhanced pain ratings compared to the presentation of painful stimuli alone. It may be that presentation of visual stimuli causes an unspecific enhancement of arousal, which in turn enhances the perceived intensity of sensory inputs. Accordingly, the absence of a pain rating enhancement in the bimodal $P_{high}V_{low}$ compared to the

unimodal P_{high} condition may be linked to the perceived strong intensity of P_{high} stimuli, which is not further enhanced by a weak visual input. Supporting this notion, we have recently observed that painful electrical stimuli were rated as being more painful when accompanied by pictures of emotional as compared to neutral faces (Senkowski et al., 2011a). Another recent study showed that viewing a needle pricking a hand compared to viewing a hand alone leads to enhanced pain ratings to concurrently presented painful stimuli (Höfle et al., 2012). The authors also reported enhanced pupil dilation in response to the presentation of the needle prick, suggesting that this condition led to an enhancement of arousal. While this assumption requires further empirical testing, it is possible that intensity dependent influence of visual input on pain perception is linked to modulation of unspecific arousal. Our finding of stronger visual biasing effects on low compared to high intensity pain stimuli, however, is well in line with the principle of IE.

Beta-band activity

Multisensory interactions in BBA at the medio-central scalp, encompassing regions of the sensorimotor cortex, followed the pattern of IE (Fig. 4). The suppression of BBA for the differences between bimodal and unimodal stimuli was stronger when the painful input was low compared to when it was high in intensity. The topography of this effect (Fig. 4) as well as the observation of similar responses to pain only stimuli (Fig. 2) suggests an involvement of sensorimotor areas. Neural responses to painful stimuli in sensorimotor cortex have been linked to the sensory-discriminative dimension of pain perception, which reflects intensity and spatiotemporal aspects of pain (Coghill et al., 1999; Derbyshire et al., 1997; Timmermann et al., 2001). Our data suggest that processing of these aspects of pain stimuli is modulated through crossmodal interactions by contextual visual stimuli, following the principle of IE.

Another interesting finding was that multisensory interactions in BBA at posterior scalp, encompassing regions of the occipital cortex, were inversely related to visual stimulus intensity. The effect was stronger when visual contrast was low compared to when it was high in intensity. Previous work has shown IE in audiovisual processing both for ERPs over occipital visual areas (Senkowski et al., 2011b; Stevenson et al., 2012) as well as for hemodynamic responses in superior temporal sulcus (Werner and Noppeney, 2010). Furthermore, using fMRI, Kim et al. (2012) found a pattern of IE for integrative visuotactile processing in occipital cortex. Thus, our finding suggests that painful stimuli modulate suppression of BBA as an inverse function of visual stimulus intensity.

Also of interest is the observation that multisensory interactions in oscillatory responses were found in the beta band. In line with previous EEG studies using visual and painful stimuli (Raij et al., 2004; Ploner et al., 2006), beta-band activity showed a pronounced decrease after stimulus presentation which lasted from 200 to 400 ms and showed maximum activities at medio-central and posterior scalp regions. Similar topographies and spectrotemporal characteristics have also been found in studies using tactile stimulation. Cheyne et al. (2003) observed suppression of 8–30 Hz activity over sensorimotor regions in response to tactile stimulation. Using MEG, Bauer et al. (2009) reported widespread suppression of beta-band activity over medio-central and posterior areas after visuotactile stimulation. Beta-band suppression has been often interpreted as a neural signature of activation in sensorimotor areas (Neuper et al., 2006; Pfurtscheller and Lopes, 1999). For instance, Raij et al. (2004) reported faster reaction times for motor responses that are executed during periods of beta-band suppression compared to motor responses executed before beta-band suppression. In addition, Stancak et al. (2005) found an increase in coherence between sensorimotor BBA and peripheral muscle activity after painful stimulation, supporting the functional relevance of pain-induced BBA suppression for motor responses. Recently, Engel and Fries (2010) suggested a role for BBA in signaling the brain's 'status quo'. The authors suggested a steady level of BBA when there is no change in the cognitive or perceptual set. A decrease of BBA is predicted when the current state is disrupted by a novel or unexpected stimulus. The effects on BBA suppression in the present study may thus reflect the alerting function of pain, which demands attention and urges to react.

The observed effects on BBA suppression possibly might also reflect the preparation of the behavioral response associated with the pain rating. Participants rated the intensity and unpleasantness of painful stimuli, which were applied to their left index finger, with a joystick in their right hand Thus, if the BBA effects in the present study would be primarily related to the preparation of the pain ratings, one would expect to find the most robust differences between bimodal PV and combined visual and painful trials over ipsilateral (i.e. left) sensorimotor regions. However, the strongest differences between PV and combined visual and painful trials were found over contralateral sensorimotor regions (Supplementary Fig. 1B). This suggests that differences in motor preparation associated with the pain ratings are not likely to account for the observed effects of stimulus intensity on BBA suppression.

Gamma-band activity

GBA increased as a function of stimulus intensity (Fig. 5; Table 1). Although the overall electrical stimulus intensity was the same for both bimodal and combined unimodal trials, GBA as well as pain ratings were, on average, higher in bimodal conditions compared to the corresponding unimodal conditions. Thus, GBA reflects the general differences in subjective pain intensities between bimodal and combined unimodal trials. This finding is in line with numerous recent studies on pain processing and pain perception (Gross et al., 2007; Schulz et al., 2011; Zhang et al., 2012). Using MEG, Gross et al. (2007) found GBA in the primary somatosensory cortex to follow physical stimulus intensity as well as subjective pain intensity ratings. Similarly, Zhang et al. (2012) showed that GBA reflects subjective pain intensity, irrespectively of the overall stimulus saliency. Moreover, using a classifier trained on single-trial data, Schulz et al. (2011) predicted individual's sensitivity to pain from a combination of pain-evoked lower frequency-band (1–20 Hz) and induced gamma-band activity. Adding to these previous studies, our results provide further evidence for the role of GBA in pain processing. Interestingly, there were no significant differences in multisensory interactions between the different stimulation conditions. GBA was generally higher for bimodal compared to combined unimodal stimuli. This suggests that GBA does not directly reflect the inverse relationship between stimulus intensity and pain processing, as obtained in pain ratings.

Event-related potentials

Multisensory interactions in right-central ERPs, encompassing the N2 component, showed a pattern of IE (Fig. 6B). ERP amplitude differences between bimodal and unimodal conditions were larger, i.e. more negative, when the painful input was low compared to when it was high in intensity. Our finding of IE in ERPs fits with a number of previous studies investigating IE in human behavioral and neural responses to non-painful multisensory stimuli. Recently, Senkowski et al. (2011b) demonstrated IE in ERPs following basic, semantically meaningless audiovisual stimulation. Using naturalistic audiovisual speech stimuli, Stevenson et al. (2012) observed IE effects in ERPs at similar latencies as observed in the present study.

Previous studies have linked the N2/P2 complex to the processing of pain (Bromm and Lorenz, 1998; Kakigi et al., 2000) and to the subjectively perceived intensity of painful input (Bromm, 1987). Interestingly, recent work has suggested that the N2/P2 complex may primarily relate to more general aspects of the presented stimuli, like saliency (Iannetti et al., 2008b; Mouraux and Iannetti, 2009) or

attention directed to a novel stimulus (Legrain et al., 2009). The present study does not allow to disentangle whether the observed ERP effects relate to pain-specific or more general stimulus processing. However, irrespective of its origin, we show that the N2 component follows the principle of IE in visual-painful processing.

Potential issues when examining the principle of inverse effectiveness

Recently, potential issues concerning the principle of IE have been raised (Holmes, 2007). A major criticism was that the post-hoc conditionalization of the data based on the strength of unimodal response properties could lead to regression towards the mean. The present study circumvents this issue by defining a priori the intensities of presented stimuli. Another issue was that floor or ceiling effects in the data might contribute to the finding of IE. Based on previous work (Höfle et al., 2012; Senkowski et al., 2011b) the stimulus intensities in the present study were carefully selected not to produce floor or ceiling effects. Finally, it has been argued that the use of a relative measurement of multisensory response gain (i.e. relative percentage change compared to the summed bimodal response) may increase the likelihood of observing IE effects. To circumvent this issue, we examined the absolute multisensory response gain in the present study.

Conclusion

Our study shows that multisensory processing of visual-painful stimuli in pain intensity ratings, BBA, and ERPs follows the principle of IE. We provide evidence that integrative processing between painful and visual stimuli works in a similar way as previously reported for multisensory processing of stimuli from other sensory modalities. Moreover, our study demonstrates that spatially and temporally aligned basic visual stimuli can bias the perception of pain, even though they do not contain semantically meaningful information. Finally, our study suggests a role of beta-band suppression in pain processing. To our knowledge, the present study is the first to demonstrate that the principle of IE is applicable to the crossmodal processing of pain.

Supplementary data to this article can be found online at http://dx.doi.org/10.1016/j.neuroimage.2012.10.040.

Acknowledgments

We would like to thank Roger Zimmermann for help with the preparation of the experimental setup and Karin Deazle and Benjamin Asanov for recruitment of participants and help with data recordings. This study was supported by grants from the German Research Foundation (DFG) (SE 1859/1-2, D.S.; SFB TRR 58 B04, A.K.E.) and the European Union (ERC-2010-StG-20091209, D.S.; ERC-2010-AdG-269716, A.K.E.).

References

Babiloni, C., Babiloni, F., Carducci, F., Cincotti, F., Rosciarelli, F., Arendt-Nielsen, L., Chen, A.C.N., Rossini, P.M., 2002. Human brain oscillatory activity phase-locked to painful electrical stimulations: a multi-channel EEG study. Hum. Brain Mapp. 15, 112–123.
Bauer, M., Oostenveld, R., Fries, P., 2009. Tactile stimulation accelerates behavioral responses to visual stimuli through enhancement of occipital gamma-band activity. Vision Res. 49, 931–942.
Bromm, B., 1987. Assessment of analgesia by evoked cerebral potential measurements in humans. Postgrad. Med. J. 63 (Suppl. 3), 9–13.
Bromm, B., Meier, W., 1984. The intracutaneous stimulus: a new pain model for algesimetric studies. Methods Find. Exp. Clin. Pharmacol. 6, 405–410.
Bromm, B., Lorenz, J., 1998. Neurophysiological evaluation of pain. Electroencephalogr. Clin. Neurophysiol. 107, 227–253.
Busse, L., Woldorff, M.G., 2003. The ERP omitted stimulus response to "no-stim" events and its implications for fast-rate event-related fMRI designs. NeuroImage 18, 856–864.
Cappe, C., Thelen, A., Romei, V., Thut, G., Murray, M.M., 2012. Looming signals reveal synergistic principles of multisensory integration. J. Neurosci. 32, 1171–1182.
Cheyne, D., Gaetz, W., Garnero, L., Lachaux, J.-P., Ducorps, A., Schwartz, D., Varela, F.J., 2003. Neuromagnetic imaging of cortical oscillations accompanying tactile stimulation. Brain Res. Cogn. Brain Res. 17, 599–611.
Coghill, R.C., Sang, C.N., Maisog, J.M., Iadarola, M.J., Wattendorf, E., Westermann, B., Fiedler, K., Kaza, E., Lotze, M., Celio, R., Maisog, J.M.A., 1999. Pain intensity processing within the human brain: a bilateral, distributed mechanism. J. Neurophysiol. 1934–1943.
Corneil, B.D., Wanrooij, M.V., Munoz, D.P., Opstal, A.J.V., Pluta, S.R., Rowland, B.A., Stanford, T.R., Stein, B.E., 2002. Auditory–visual interactions subserving goal-directed saccades in a complex scene. J. Neurophysiol. 438–454.
Delorme, A., Makeig, S., 2004. EEGLAB: an open source toolbox for analysis of single-trial EEG dynamics including independent component analysis. J. Neurosci. Methods 134, 9–21.
Derbyshire, S.W., Jones, A.K., Gyulai, F., Clark, S., Townsend, D., Firestone, L.L., 1997. Pain processing during three levels of noxious stimulation produces differential patterns of central activity. Pain 73, 431–445.
Diederich, A., Colonius, H., 2004. Bimodal and trimodal multisensory enhancement: effects of stimulus onset and intensity on reaction time. Percept. Psychophys. 66, 1388–1404.
Domnick, C., Hauck, M., Casey, K.L., Engel, A.K., Lorenz, J., 2009. C-fiber-related EEG-oscillations induced by laser radiant heat stimulation of capsaicin-treated skin. J. Pain Res. 2, 49–56.
Engel, A.K., Fries, P., 2010. Beta-band oscillations-signalling the status quo? Curr. Opin. Neurobiol. 20, 156–165.
Frassinetti, F., Bolognini, N., Làdavas, E., 2002. Enhancement of visual perception by crossmodal visuo-auditory interaction. Exp. Brain Res. 147, 332–343.
Giard, M.H., Peronnet, F., 1999. Auditory–visual integration during multimodal object recognition in humans: a behavioral and electrophysiological study. J. Cogn. Neurosci. 11, 473–490.
Gondan, M., Niederhaus, B., Rösler, F., Röder, B., 2005. Multisensory processing in the redundant-target effect: a behavioral and event-related potential study. Percept. Psychophys. 67, 713–726.
Gross, J., Schnitzler, A., Timmermann, L., Ploner, M., 2007. Gamma oscillations in human primary somatosensory cortex reflect pain perception. PLoS Biol. 5, e133.
Hauck, M., Lorenz, J., Engel, A.K., 2007. Attention to painful stimulation enhances gamma-band activity and synchronization in human sensorimotor cortex. J. Neurosci. 27, 9270–9277.
Hauck, M., Lorenz, J., Engel, A.K., 2008. Role of synchronized oscillatory brain activity for human pain perception. Rev. Neurosci. 19, 441–450.
Höfle, M., Hauck, M., Engel, A.K., Senkowski, D., 2012. Viewing a needle pricking a hand that you perceive as yours enhances unpleasantness of pain. Pain 153, 1074–1081.
Holmes, N.P., 2007. The law of inverse effectiveness in neurons and behaviour: multisensory integration versus normal variability. Neuropsychologia 45, 3340–3345.
Iannetti, G.D., Hughes, N.P., Lee, M.C., Mouraux, A., 2008a. Determinants of laser-evoked EEG responses: pain perception or stimulus saliency? J. Neurophysiol. 815–828.
Kakigi, R., Watanabe, S., Yamasaki, H., 2000. Pain-related somatosensory evoked potentials. J. Clin. Neurophysiol. 17, 295–308.
Kayser, C., Petkov, C.I., Logothetis, N.K., 2008. Visual modulation of neurons in auditory cortex. Cereb. Cortex 18, 1560–1574.
Kim, S., Stevenson, R.A., James, T.W., 2012. Visuo-haptic neuronal convergence demonstrated with an inversely effective pattern of BOLD activation. J. Cogn. Neurosci. 830–842.
Legrain, V., Perchet, C., García-Larrea, L., 2009. Involuntary orienting of attention to nociceptive events: neural and behavioral signatures. J. Neurophysiol. 102, 2423–2434.
Mancini, F., Longo, M., Canzoneri, E., Vallar, G., Haggard, P., accepted for publication. Changes in cortical oscillations linked to multisensory modulation of nociception. Eur. J. Neurosci.
Mitra, P.P., Pesaran, B., 1999. Analysis of dynamic brain imaging data. Biophys. J. 76, 691–708.
Molholm, S., Ritter, W., Murray, M.M., Javitt, D.C., Schroeder, C.E., Foxe, J.J., 2002. Multisensory auditory–visual interactions during early sensory processing in humans: a high-density electrical mapping study. Brain Res. Cogn. Brain Res. 14, 115–128.
Mouraux, A., Iannetti, G., 2009. Nociceptive laser-evoked brain potentials do not reflect nociceptive-specific neural activity. J. Neurophysiol. 101, 3258–3269.
Mouraux, A., Guérit, J., Plaghki, L., 2003. Non-phase locked electroencephalogram (EEG) responses to CO_2 laser skin stimulations may reflect central interactions between A∂- and C-fibre afferent volleys. Clin. Neurophysiol. 114, 710–722.
Mouraux, A., Iannetti, G.D., Plaghki, L., 2010. Low intensity intra-epidermal electrical stimulation can activate Aδ-nociceptors selectively. Pain 150, 199–207.
Murray, M.M., Molholm, S., Michel, C.M., Heslenfeld, D.J., Ritter, W., Javitt, D.C., Schroeder, C.E., Foxe, J.J., 2005. Grabbing your ear: rapid auditory–somatosensory multisensory interactions in low-level sensory cortices are not constrained by stimulus alignment. Cereb. Cortex 15, 963–974.
Nasri, N., Beno, N., Septier, C., Salles, C., Thomas-Danguin, T., 2011. Cross-modal interactions between taste and smell: odour-induced saltiness enhancement depends on salt level. Food Qual. Prefer. 22, 678–682.
Neuper, C., Wörtz, M., Pfurtscheller, G., 2006. ERD/ERS patterns reflecting sensorimotor activation and deactivation. Prog. Brain Res. 159, 211–222.
Odgaard, E.C., Arieh, Y., Marks, L.E., 2004. Brighter noise: sensory enhancement of perceived loudness by concurrent visual stimulation. Cogn. Affect. Behav. Neurosci. 4, 127–132.
Oostenveld, R., Fries, P., Maris, E., Schoffelen, J.-M., 2011. FieldTrip: open source software for advanced analysis of MEG, EEG, and invasive electrophysiological data. Comput. Intell. Neurosci. 2011, 156869.
Perrin, F., Pernier, J., Bertrand, O., Echallier, J.F., 1989. Spherical splines for scalp potential and current density mapping. Electroencephalogr. Clin. Neurophysiol. 72, 184–187.
Pfurtscheller, G., Lopes, F.H., 1999. Event-related EEG/MEG synchronization and desynchronization: basic principles. Clin. Neurophysiol. 110, 1842–1857.
Ploner, M., Gross, J., Timmermann, L., Pollok, B., Schnitzler, A., 2006. Pain suppresses spontaneous brain rhythms. Cereb. Cortex 16, 537–540.

Rach, S., Diederich, A., Colonius, H., 2011. On quantifying multisensory interaction effects in reaction time and detection rate. Psychol. Res. 75, 77–94.
Raij, T.T., Forss, N., Stancak, A., Hari, R., 2004. Modulation of motor-cortex oscillatory activity by painful A-delta-and C-fiber stimuli. NeuroImage 23, 569–573.
Ross, L.A., Saint-Amour, D., Leavitt, V.M., Javitt, D.C., Foxe, J.J., 2007. Do you see what I am saying? Exploring visual enhancement of speech comprehension in noisy environments. Cereb. Cortex 17, 1147–1153.
Schneider, T.R., Debener, S., Oostenveld, R., Engel, A.K., 2008. Enhanced EEG gamma-band activity reflects multisensory semantic matching in visual-to-auditory object priming. NeuroImage 42, 1244–1254.
Schneider, T.R., Lorenz, S., Senkowski, D., Engel, A.K., 2011. Gamma-band activity as a signature for cross-modal priming of auditory object recognition by active haptic exploration. J. Neurosci. 31, 2502–2510.
Schulz, E., Zherdin, A., Tiemann, L., Plant, C., Ploner, M., 2011. Decoding an individual's sensitivity to pain from the multivariate analysis of EEG data. Cerebral Cortex 22 (5), 1118–1123.
Senkowski, D., Gomez-Ramirez, M., Lakatos, P., Wylie, G.R., Molholm, S., Schroeder, C.E., Foxe, J.J., 2007a. Multisensory processing and oscillatory activity: analyzing non-linear electrophysiological measures in humans and simians. Exp. Brain Res. 177, 184–195.
Senkowski, D., Talsma, D., Grigutsch, M., Herrmann, C.S., Woldorff, M.G., 2007b. Good times for multisensory integration: effects of the precision of temporal synchrony as revealed by gamma-band oscillations. Neuropsychologia 45, 561–571.
Senkowski, D., Schneider, T.R., Foxe, J.J., Engel, A.K., 2008. Crossmodal binding through neural coherence: implications for multisensory processing. Trends Neurosci. 31, 401–409.
Senkowski, D., Kautz, J., Hauck, M., Zimmermann, R., Engel, A.K., 2011a. Emotional facial expressions modulate pain-induced beta and gamma oscillations in sensorimotor cortex. J. Neurosci. 31, 14542–14550.
Senkowski, D., Saint-Amour, D., Höfle, M., Foxe, J.J., 2011b. Multisensory interactions in early evoked brain activity follow the principle of inverse effectiveness. NeuroImage 56, 2200–2208.
Stancak, A., Raij, T.T., Pohja, M., Forss, N., Hari, R., 2005. Oscillatory motor cortex-muscle coupling during painful laser and nonpainful tactile stimulation. NeuroImage 26, 793–800.
Stein, B.E., Meredith, M.A., 1993. The Merging of the Senses. MIT Press.
Stein, B.E., Stanford, T.R., 2008. Multisensory integration: current issues from the perspective of the single neuron. Nat. Rev. Neurosci. 9, 255–266.
Stein, B., London, N., Wilkinson, L., Price, D., 1996. Enhancement of perceived visual intensity by auditory stimuli: a psychophysical analysis. J. Cogn. Neurosci. 497–506.
Stevenson, R.A., James, T.W., 2009. Audiovisual integration in human superior temporal sulcus: inverse effectiveness and the neural processing of speech and object recognition. NeuroImage 44, 1210–1223.
Stevenson, R.A., Bushmakin, M., James, T.W., 2012. Inverse effectiveness and multisensory interactions in visual event-related potentials with audiovisual speech. Brain Topogr. 25 (3), 308–326.
Talsma, D., Woldorff, M.G., 2005. Selective attention and multisensory integration: multiple phases of effects on the evoked brain activity. J. Cogn. Neurosci. 17, 1098–1114.
Teder-Sälejärvi, W.A., McDonald, J.J., Di Russo, F., Hillyard, S.A., 2002. An analysis of audio-visual crossmodal integration by means of event-related potential (ERP) recordings. Brain Res. Cogn. Brain Res. 14, 106–114.
Tiemann, L., Schulz, E., Gross, J., Ploner, M., 2010. Gamma oscillations as a neuronal correlate of the attentional effects of pain. Pain 150, 302–308.
Timmermann, L., Ploner, M., Haucke, K., Schmitz, F., Baltissen, R., Schnitzler, A., 2001. Differential coding of pain intensity in the human primary and secondary somatosensory cortex. J. Neurophysiol. 86, 1499–1503.
Trenner, M.U., Heekeren, H.R., Bauer, M., Rössner, K., Wenzel, R., Villringer, A., Fahle, M., 2008. What happens in between? Human oscillatory brain activity related to crossmodal spatial cueing. PLoS One 3, e1467.
Valeriani, M., Betti, V., Le Pera, D., De Armas, L., Miliucci, R., Restuccia, D., Avenanti, A., Aglioti, S.M., 2008. Seeing the pain of others while being in pain: a laser-evoked potentials study. NeuroImage 40, 1419–1428.
Werner, S., Noppeney, U., 2010. Superadditive responses in superior temporal sulcus predict audiovisual benefits in object categorization. Cereb. Cortex 20, 1829–1842.
Woldorff, M., 1993. Distortion of ERP averages due to overlap from temporally adjacent ERPs: analysis and correction. Psychophysiology 30, 98–119.
Zhang, Z.G., Hu, L., Hung, Y.S., Mouraux, A., Iannetti, G.D., 2012. Gamma-band oscillations in the primary somatosensory cortex—a direct and obligatory correlate of subjective pain intensity. J. Neurosci. 32 (22), 7429–7438.